

# Journal Pre-proof

Facilitating structural elucidation of small environmental solutes in RPLC-HRMS by retention index prediction

Ardiana Kajtazi, Giacomo Russo, Kristina Wicht, Hamed Eghbali, Frédéric Lynen



PII: S0045-6535(23)01628-4

DOI: <https://doi.org/10.1016/j.chemosphere.2023.139361>

Reference: CHEM 139361

To appear in: *ECSN*

Received Date: 14 March 2023

Revised Date: 6 June 2023

Accepted Date: 26 June 2023

Please cite this article as: Kajtazi, A., Russo, G., Wicht, K., Eghbali, H., Lynen, Fr  ., Facilitating structural elucidation of small environmental solutes in RPLC-HRMS by retention index prediction, *Chemosphere* (2023), doi: <https://doi.org/10.1016/j.chemosphere.2023.139361>.

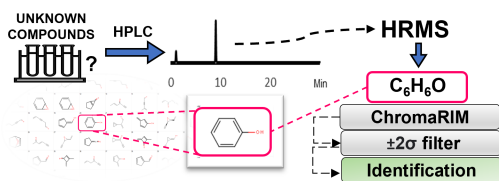
This is a PDF file of an article that has undergone enhancements after acceptance, such as the addition of a cover page and metadata, and formatting for readability, but it is not yet the definitive version of record. This version will undergo additional copyediting, typesetting and review before it is published in its final form, but we are providing this version to give early visibility of the article. Please note that, during the production process, errors may be discovered which could affect the content, and all legal disclaimers that apply to the journal pertain.

  2023 Published by Elsevier Ltd.

### **Author Contributions**

**Ardiana Kajtazi:** Conceptualization, Visualization, Methodology, Software, Investigation, Formal analysis, Writing - Original Draft; **Giacomo Russo:** Validation, Writing - Review & Editing; **Kristina Wicht:** Investigation; **Hamed Eghbali:** Supervision; **Frédéric Lynen:** Conceptualization, Visualization, Supervision, Writing - Review & Editing.

Journal Pre-proof



Journal Pre-proof

1 **Facilitating structural elucidation of small environmental solutes**  
2 **in RPLC-HRMS by retention index prediction**

3 Ardiana Kajtazi<sup>1</sup>, Giacomo Russo<sup>2</sup>, Kristina Wicht<sup>1</sup>, Hamed Eghbali<sup>3</sup>, Frédéric Lynen<sup>1\*</sup>

4 <sup>1</sup>Separation Science Group, Department of Organic and Macromolecular Chemistry, Ghent University,  
5 Krijgslaan 281 S4bis, B-9000 Ghent, Belgium

6 <sup>2</sup>School of Applied Sciences, Sighthill Campus, Edinburgh Napier University, 9 Sighthill Ct, EH11  
7 4BN, Edinburgh, United Kingdom

8 <sup>3</sup>Packaging and Specialty Plastics R&D, Dow Benelux B.V., Terneuzen, 4530 AA, the Netherlands

9 \*Correspondance: [frederic.lynen@ugent.be](mailto:frederic.lynen@ugent.be)

**10 Abstract**

11 Implementing effective environmental management strategies requires a comprehensive  
12 understanding of the chemical composition of environmental pollutants, particularly in complex  
13 mixtures. Utilizing innovative analytical techniques, such as high-resolution mass spectrometry and  
14 predictive retention index models, can provide valuable insights into the molecular structures of  
15 environmental contaminants. Liquid Chromatography-High-Resolution Mass Spectrometry is a  
16 powerful tool for the identification of isomeric structures in complex samples. However, there are some  
17 limitations that can prevent accurate isomeric structure identification, particularly in cases where the  
18 isomers have similar mass and fragmentation patterns. Liquid chromatographic retention, determined  
19 by the size, shape, and polarity of the analyte and its interactions with the stationary phase, contains  
20 valuable 3D structural information that is vastly underutilized. Therefore, a predictive retention index  
21 model is developed which is transferrable to LC-HRMS systems and can assist in the structural  
22 elucidation of unknowns. The approach is currently restricted to carbon, hydrogen, and oxygen-based  
23 molecules  $<500 \text{ g mol}^{-1}$ . The methodology facilitates the acceptance of accurate structural formulas and  
24 the exclusion of erroneous hypothetical structural representations by leveraging retention time  
25 estimations, thereby providing a permissible tolerance range for a given elemental composition and  
26 experimental retention time. This approach serves as a proof of concept for the development of a  
27 Quantitative Structure-Retention Relationship model using a generic gradient LC approach. The use of  
28 a widely used reversed-phase (U)HPLC column and a relatively large set of training (101) and test  
29 compounds (14) demonstrates the feasibility and potential applicability of this approach for predicting  
30 the retention behaviour of compounds in complex mixtures. By providing a standard operating  
31 procedure, this approach can be easily replicated and applied to various analytical challenges, further  
32 supporting its potential for broader implementation.

33

34 **KEYWORDS:** *HPLC-HRMS, Quantitative Structure- Retention Relationship model, In silico*  
35 *prediction, Retention index, Structural elucidation.*

## 36 1. Introduction

37 Since the onset of this millennium, the ability of high-resolution mass spectrometry to elucidate the  
38 elemental composition of unknown organic molecules has been steadily increasing (Boiteau et al.,  
39 2018; De Vijlder et al., 2018). The high mass accuracy in combination with isotope distribution  
40 assessment allows now the minimization of a vast number of possible corresponding elemental  
41 compositions down to a manageable few. The correct atomic composition can then in many cases fairly  
42 easily be obtained based on chemical reasonability, stability, and relevance (De Vijlder et al., 2018).  
43 Additional information can and should then also be obtained via MS/MS fragmentation analysis  
44 whereby the elemental composition of the daughter ions should be a logical fragment of the parent  
45 compound. Because the current instrumentation certainly allows successful implementation of this  
46 protocol up to molecular weights of at least  $500 \text{ g mol}^{-1}$ , the more challenging part of the identification  
47 process is largely to be found in the subsequent structural elucidation problem (Boiteau et al., 2018; De  
48 Vijlder et al., 2018; Liu et al., 2019).

49 The identification of previously known molecules via LC-MS can be performed if authentic  
50 standards are available and/or if they appear in accessible public databases (such as METLIN,  
51 PubChem, and Mass Bank) (Domingo-Almenara et al., 2019; Horai et al., 2010; Wen et al., 2018a).  
52 The ensuing identification is then also strongly reliant on mass fragmentography, which can, due to the  
53 selectivity of HRMS, allow for the correct identification of the molecule or type of molecule. While  
54 this does not exclude the possibility of misidentification due to positional isomer confusion, typically it  
55 can be distinguished via chromatographic retention or by ion mobility measurements, whereby further  
56 increased reliability is obtained when the information from different separation modes or conditions is  
57 combined (Eugster et al., 2014; Kumari et al., 2011).

58 By contrast, de novo structural elucidation of a priori truly unknown compounds, non-annotated in  
59 databases, but for which an elemental composition can be obtained by HRMS, is more problematic  
60 (Kumari et al., 2011). This would be typically solved via the combined implementation of various  
61 spectroscopic techniques with a particularly strong emphasis on nuclear magnetic resonance  
62 spectroscopy (NMR). NMR remains, however, limited due to the at least  $> 0.1 \text{ mg}$  analyte quantity and

63 purity prerequisites, compelling the implementation of multi-repetitive tedious and costly preparative  
64 compound fractionation and purification protocols, prior to the spectroscopy (Witting and Böcker,  
65 2020). While this is a well-nurtured approach in chemical or drug development processes, preparative  
66 compound purification in life- or environmental sciences are often not feasible due to the too small  
67 concentrations and high sample complexity usually involved (Szucs et al., 2021). Additionally, while  
68 NMR is the most powerful tool for structural elucidation, the expert nature of the techniques and the  
69 lack of specialist-free fully automated structural elucidations algorithms add other hurdles to the  
70 challenge (Witting and Böcker, 2020). Another problem with the analysis of unknown solutes is that  
71 often they are confused with known related compounds in the databases, whereby obtaining definitive  
72 proof of the actual structure is difficult. Therefore, there is a strong need for the development of  
73 additional tools allowing to gather structural information of solutes, also when they appear at trace  
74 levels that are only detectable by mass spectrometry (Aalizadeh et al., 2021; Boiteau et al., 2018; Cui  
75 et al., 2018; Liu et al., 2019).

76 While the available chromatographic retention information in LC-MS data has been for a long time  
77 underused for such purposes, its increased implementation is now gradually emerging to assist in this  
78 elucidation process (Gritti, 2023; Zheng et al., 2018). The main challenge therein is that unfortunately  
79 chromatographic retention as it is today cannot directly be related to the unambiguous and discrete  
80 molecular characteristics hence leading to specific, “easily” understandable, and predictable behavior.  
81 This comprising the fragmentation, absorbance or excitation processes observed in mass spectrometry,  
82 UV/IR or NMR spectroscopy, respectively (Aalizadeh et al., 2021; Sagandykova and Buszewski, 2021).  
83 On the other hand, the retention mechanism of e.g., the reversed phase LC mode is intuitively  
84 understood by any chemist. Because also the purity of the stationary phases has concomitantly been  
85 improving over time this has led to the many contemporary robust reversed phase methods ubiquitously  
86 used in the strictest validated analytical environments (Haddad et al., 2021a). Hence, the composition,  
87 structural formula, shape and e.g., the solvation of a molecular structure are all reflected through a  
88 particular resulting retention time. The latter can therefore also be considered a molecular characteristic  
89 which offers a powerful tool in the search for the structural formula for a given elemental composition.

90 Much research has been performed with respect to the prediction of molecular retention time for a  
91 given structural formula for applications such as swifter method development, suitable column selection  
92 and for enhanced compound elucidation within specific compound classes (Meshref et al., 2020;  
93 Randazzo et al., 2016a; Wen et al., 2018b; Xu et al., 2023). Various retention models were thereby  
94 introduced for Reversed-Phase Liquid Chromatography (RPLC), Hydrophilic Interaction Liquid  
95 Chromatography (HILIC), and Ion Chromatography (IC) separation modes (Haddad et al., 2021a;  
96 Randazzo et al., 2016a). Such algorithms are also increasingly successfully implemented for the  
97 prediction of the retention time of a range of specific groups of analytes, such as lipids (Aichele et al.,  
98 2015; Zheng et al., 2018), steroids (Randazzo et al., 2016a), peptides (Bouwmeester et al., 2021; Dorfer  
99 et al., 2018), proteins (Palmlad et al., 2004), and more.

100 When predicting the chromatographic behavior, the Quantitative Structure-Retention Relationship  
101 (QSRR) modelling has often offered a propitious solution in building a promising predictive model  
102 (Kaliszan, 1993; Wen et al., 2018a). These mathematical models characterize retention relationships of  
103 molecules and have been applied for the aforementioned chromatographic separation techniques, for  
104 more than four decades (Amos et al., 2018). In these studies, the model is often used to predict the  
105 retention of a target group of compounds to acquire either faster identification and/or greater  
106 comprehension of the retention mechanism (Héberger, 2007). The first step involves collecting the  
107 experimental retention time of a known training set, such as to be able to build a predictive model that  
108 relates retention to the most relevant and broadly applicable molecular characteristics of the training set  
109 (Haddad et al., 2021b). Such methods have also been used to predict a variety of molecular  
110 characteristics such as retention time (RT) (Ma et al., 2018; Randazzo et al., 2016b; Szucs et al., 2021;  
111 Wen et al., 2019; Yang et al., 2021), retention factor ( $k$ ) (Ruggieri et al., 2005a),  $\log K_w$  (Codesido et  
112 al., 2019),  $\log P$  (Datta et al., 2021),  $\log D$  (Köhler et al., 2023), and ability to permeate through  
113 biological membranes (Russo et al., 2017). Recently the QSRR approach has been increasingly used to  
114 prove or disprove the composition of classes of molecules characterized by their modular nature such  
115 as peptides or lipids in combination with HRMS/MS (Bouwmeester et al., 2021; Dorfer et al., 2018;  
116 Hutchins et al., 2018; Ma et al., 2018; Tiwary et al., 2019). The challenges which have thus far refrained



117 this approach from becoming universally applicable or broadly applied are multifaceted and appear  
118 mainly related to standardization and transferability.

119 On the one hand, unfortunately, much QSRR work has also often been performed on RPLC columns  
120 or with chromatographic conditions which are less broadly used. Additionally, the transferability of the  
121 resulting retention data to any HPLC instrument type is as important. Considering the notoriously  
122 difficult method transfer between different instruments or geographic locations, predictive QSRR  
123 models based on retention time or even retention factor are therefore also inherently limited (Haddad et  
124 al., 2021a). Additionally, the absence of easily accessible open source information and of fully  
125 transferable workflows has also been hindering the development of a gold standard for LC-HRMS based  
126 structural elucidation of unknown organic solutes for which an elemental composition has been  
127 obtained. Today high-resolution mass spectrometry offers a powerful tool for reasonably reliable  
128 prediction of the elemental composition of complete unknowns. Combinations with QSRR then allows  
129 translation of the latter into all possible hypothetical structural formulas, for which the corresponding  
130 predicted retention (time, factor, or index) can be compared with the experimental retention. This allows  
131 removing of a large number of impossible structural formulas for a given retention time.

132 The proposed research aims to enhance the structural elucidation of unknown environmental solutes  
133 with a molecular weight of less than  $500 \text{ g mol}^{-1}$  ( $\text{MW} < 500 \text{ g mol}^{-1}$ ) that contain carbon, hydrogen, or  
134 oxygen atoms. To achieve this, the study presents a novel approach that uniquely combines HRMS and  
135 retention information to build a predictive Chromatographic Retention Index Model (ChromaRIM). The  
136 transferability of the strategy is maximized through the translation of the retention information into  
137 retention indices (RI) on one of the most used stationary and mobile phase combinations, with a gradient  
138 spanning the entire elution range. The methodology is tested with known and unknown organic solutes  
139 of wastewater treatment relevance.

## 140 **2. Experimental**

### 141 **2.1 Chemicals and reagents**

142 HPLC grade acetonitrile (MeCN), methanol (MeOH), and ethanol (EtOH) were obtained from  
143 Sigma–Aldrich (Steinheim, Germany). Milli-Q grade water ( $18.2 \text{ m}\Omega \text{ cm}^{-1}$ ) was purified and deionized

144 in-house by a Milli-Q plus instrument from Millipore (Bedford, USA). Formic acid (FA), 99% purity,  
145 was supplied from Sigma–Aldrich (Steinheim, Germany). The 115 neat standard compounds (purity >  
146 98%) were obtained from TCI EUROPE N.V. (Zwijndrecht, Belgium) and Sigma–Aldrich (Steinheim,  
147 Germany).

## 148 **2.2 Sample preparation**

149 Stock solutions of training and test compounds were prepared in concentrations from 1-10 mg mL<sup>-1</sup>  
150 in MeCN, EtOH, and MeOH, depending on their solubility. Once the stock solutions were prepared,  
151 they were stored in the fridge or freezer (4 °C/ -18 °C). Standard working solutions were diluted to the  
152 concentration of 1-20 µg mL<sup>-1</sup> in 60:40 (Milli-Q water: Organic solvent) and prepared on the day of  
153 analysis.

## 154 **2.3 Instrumentation and method development**

155 Chromatographic separation was performed on a 1200 series HPLC system (Agilent Technologies,  
156 Waldbronn, Germany). The system was constructed out of a 1200 binary pump equipped with a 1200  
157 degasser, a 1200 auto injector, and a 1200 variable wavelength detector (VWD) equipped with a 2 µL  
158 microflow cell. RP-LC measurements were performed on a Kinetex Core-shell C18 2.6 µm, 150 x 2.1  
159 mm (Phenomenex, Torrance, CA, USA) with an optimal flow rate of 400 µL min<sup>-1</sup>. The latter was  
160 determined by measuring a reference test mixture isocratically 60:40 (Milli-Q: MeCN) at different flow  
161 rates allowing for plate numbers (N) > 27 000. The LC mobile phase, (A) Milli-Q grade water (18.2  
162 mΩ cm<sup>-1</sup>) and (B) MeCN, were both prepared with 0.1% of FA. Injection volume was 2 µL and the  
163 detection for all analytes was recorded at 210 nm, whereas for ketone reference mixture at 280 nm. The  
164 column temperature was kept at 30 °C during all analyses. To obtain the most general approach methods  
165 were operated from 5-95% (B) in 1) 10 min, 2) 20 min and 3) 40 min followed by re-equilibration with  
166 5% B for the next 10 min. To test the reproducibility and repeatability of the data, these 3 separation  
167 methods were performed under the above-listed conditions with random selection of 60 compounds,  
168 with differentiation in the linear gradient (Table S2). To generate the predictive model, method 2 was  
169 used for further calculations. Full MS (Section S7) was obtained using Q Exactive Orbitrap (Thermo  
170 Fisher Scientific). Scan range was 50-500 m/z, Automatic Gain Control (AGC) target was 1e6,

171 Maximum IT was set to 100 ms, and the resolution was 280 000. Detailed ESI parameters for positive  
172 and negative mode can be found in Table S10.

#### 173 **2.4 Data collection and molecular descriptor selection**

174 The retention times of all compounds were measured in triplicate and intra- and inter-repeatability  
175 were calculated. Subsequently the corresponding RI were calculated according to Kovats RI method  
176 usually applied in gradient gas chromatography (Equation SE1). The structures of all compounds were  
177 transferred into a Simplified Molecular Input Line Entry System (SMILES) format using ChemDraw  
178 and the file was imported as such in the free (of charge) website “Online chemical database” to calculate  
179 molecular descriptors of choice using the tool DescriptorsCalculator. A total number of 1879 molecular  
180 descriptors were used comprising (2) ALogPS descriptors (Tetko et al., 2005; “Virtual Computational  
181 Chemistry Laboratory,” n.d.) and (1877) AlvaDesc v.2.0.14 (Mauri, 2020) from which (198) 2D  
182 AlvaDesc descriptors (including constitutional descriptors, Topological indices and P\_VSA-like  
183 descriptors) and (1677) 3D AlvaDesc descriptors (comprising the following categories: Geometrical  
184 descriptors, 3D matrix-based descriptors, 3D autocorrelations, RDF descriptors, 3D-MoRSE  
185 descriptors, WHIM descriptors, GETAWAY descriptors, Randic molecular profiles, Functional group  
186 counts, 3D Atom Pairs, Charge descriptors, Molecular properties, CATS 3D, and WHALES). The value  
187 for each descriptor for each solute was calculate via AlvaDesc and exported to Excel.

#### 188 **2.5 QSRR model validation**

189 The QSRR model was calculated using VEGA ZZ 3.2.1.33 (Pedretti et al., 2021), where the  
190 experimental RI was a dependent variable and molecular descriptors were the independent variables.  
191 Pre-processing of the data was done by normalization min-max feature scaling. The initial screening of  
192 descriptors involved two steps: evaluating zero variance and conducting a single-variable regression  
193 analysis (Danishuddin and Khan, 2016). Furthermore, by evaluating the variance inflation factor (VIF),  
194 collinear descriptors were recognized and those with  $VIF > 5.00$  were disregarded. With the remaining  
195 37 descriptors the best models were calculated with both leave-one-out (LOO) cross-validation and by  
196 randomly splitting the dataset into 71:30 pairs of training and test sets in 10 trials. Lastly, the best QSRR  
197 model including 7 descriptors was used in the identification of unknown compounds by predicting their

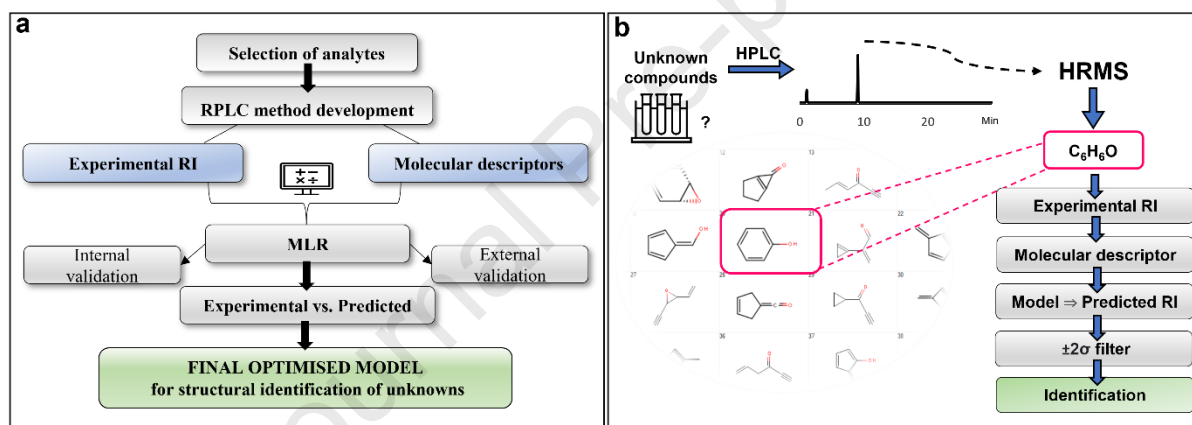
198 RI. Internal validation was statistically determined with VEGA ZZ (Table S4-S7), and external  
199 validation was done by introducing 14 external test compounds. The assessment of applicability domain  
200 (AD) was presented in the Williams plot (Figure S4) using standardized residuals and leverages. For  
201 the unknowns for which the elemental composition was known, the list of possible structures with the  
202 same molecular masses was downloaded from ChemSpider in SDF format, after which molecular  
203 descriptors were calculated in the same way. All experimental chromatograms and graphs were  
204 processed using OriginPro 9.0 (OriginLab Corporation, Northampton, MA.). Simulation  
205 chromatograms were constructed with Microsoft Excel.

### 206 **3. Results and discussion**

207 This study explores the ability of reversed phase liquid chromatography to confirm or eliminate  
208 proposed structures for organic solutes based on their elemental composition. The first phase involves  
209 the development of a gradient HPLC methodology that is broadly applicable. This methodology has the  
210 potential to be established as a standard approach for chromatography-supported structural elucidation.  
211 All retention data is therefore translated towards RI, which are subsequently used to build a QSRR  
212 model allowing to accept or reject the retention of structures in a given molecular space. Emphasis is  
213 thereby not set on the ability to predict the retention times or indices for specific molecules in the best  
214 possible way, but on the capacity of the given model to provide useful and as reliable as possible  
215 exclusion or inclusion of structural predictions for C, H, O <500 g mol<sup>-1</sup> compounds, when compared  
216 with the experimental retention of an unknown. In the second part of the work the implementation of  
217 the model is rigorously tested. It is thereby shown that it can be used to correctly accept or reject the  
218 many hypothetical structural formulas which can be drawn for a given elemental composition. Because  
219 the latter quickly leads to an astronomical number of possible structures, it is not realistic with 1D-  
220 HPLC to pinpoint only the right structure, but it does offer the ability to remove a vast number of  
221 chromatographically impossible structures for a given experimental retention time and atomic  
222 composition of an unknown solute. Assuming a robust model is used one can then select the predicted  
223 structures, eluting in the range of the experimentally obtained one, as the most probable structures of  
224 the true unknown. The latter can then be further refined via conventional exploitation of the MS/HRMS

225 info. The current ChromaRIM approach can serve as platform method for this purpose but can also be  
 226 considered as a first keystone method in multidimensional approaches whereby each added separation  
 227 dimension further refines and restrict the search zone.

228 The work is therefore subdivided into a development section comprising 1) the HPLC method  
 229 selection/development, 2) selection of the compounds and of the charted molecular space and data  
 230 collection 3) conversion to retention indices, 4) descriptor selection and attrition and 5) construction of  
 231 the most suitable QSRR model. The model is then 6) internally assessed and also tested with known  
 232 environmentally relevant solutes (for additional external consolidation) and finally 7) implemented  
 233 using the developed model. The general strategy for both the development and implementation is  
 234 represented in Figure 1A and B.



235  
 236 **Figure 1.** Representation of the workflow applied to develop the model (a) and of the proposed  
 237 implementation by the user (b).

### 238 3.1 Selecting a generic RPLC method

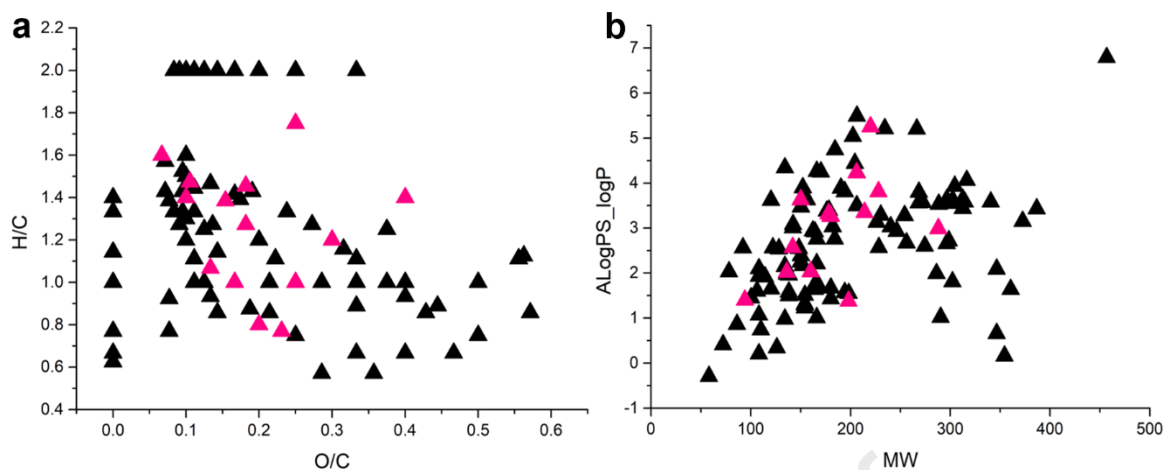
239 Proposing “the most” universal RPLC column and method is inherently ambiguous as this depends  
 240 on the geography or field of application. In this current work the implementation of  
 241 acetonitrile/water/0.1% formic acid gradients on a core-shell RPLC is proposed for this purpose. RPLC  
 242 is selected because it is the most broadly applied separation mode (Majors, 2018). A benefit of this  
 243 mode is that it can retain both neutral compounds as such, or ionized solutes via protonation (for acids)  
 244 or ion pairing (for bases) when using MS-compatible acidic conditions (e.g., with 0.1% formic acid).  
 245 Because the versatility of RPLC inherently leads to large differences in polarity of the possible analytes,

246 the use of gradients allowing both retention and elution of all solutes is essential. Acetonitrile is thereby  
247 the most suitable choice as it depicts high eluotropic strength, low viscosity, inertness, and excellent  
248 MS compatibility. A 150 x 2.1 mm ID core shell-based method was selected because it allows  
249 implementation in both HPLC and UHPLC while ensuring easy hyphenation to mass spectrometry. A  
250 core shell type of stationary phases was selected as such type is increasingly used, while being highly  
251 efficient at a lower pressure drop as compared to full porous particles (González-Ruiz et al., 2015;  
252 Tanaka and Mccalley, 2015).

### 253 **3.2 Selection of compounds as a function of the molecular space of interest**

254 Within a molecular space composed of only C, H and O up to 500 g mol<sup>-1</sup> a large number of different  
255 elemental compositions can occur, leading to billions of possible corresponding structural formulas.  
256 Selection of the most representative data set is thereby inherently ambiguous and fraught with  
257 challenges. Emphasis was therefore set on the selection of compounds allowing broad coverage of the  
258 separation space.

259 A variety of conventional C<sub>x</sub>H<sub>y</sub>O<sub>z</sub> organic solutes, pharmaceuticals, compounds of environmental  
260 concerns were selected for this purpose, such as to cover the molecular space in the best possible way.  
261 Van Krevelen plots and ALogPS\_logP vs. MW representations were used for this (Figure 2, Table S1).  
262 The former illustrates a broad coverage in the amount of unsaturations (from 1 for the ketone ladder  
263 compounds to 11 for alizarin) while spanning a fair polarity range reflected through the O/C ratio range  
264 from 0 (for e.g., toluene) up to 0.6 for 2,5 dihydroxy-benzoic acid. A reflection of the polarity and hence  
265 water solubility is also obtained through visualization of the logP's vs. the MW, where it can be seen  
266 that the logP's range from close to 0 up to 7 and in this way e.g., outspan the range of typical  
267 pharmaceutical solutes. This also covers the applicability range of gradient RPLC as more polar solutes  
268 (saccharides) would barely be retained and more apolar solutes (petrochemical compounds) require  
269 stronger elution conditions with less generic solvents. Highly oxygenated or unstable species  
270 (saccharides, peroxides, or aldehydes) were avoided due to low compound retention or stability issues  
271 involved. Additionally, the expected C, H, O, functional groups were comprised in the dataset (alcohols,  
272 carboxylic groups, ketones, esters, aromatic, linear, and branched solutes, etc.).



273

274 **Figure 2.** Representation of the (a) Van Krevelen plots (H/C vs. O/C ratio's) and of the (b)

275 ALogPS\_logP vs. MW of the 101 training set (black) and 14 test set (pink).

276 **3.3 Data collection and conversion to retention indices**

277 Although the purpose of this work was to introduce one broadly applicable gradient profile, the

278 retention of 60 solutes was also measured (in triplicate) with 3 gradient profiles spanning the full elution

279 range in 10, 20 or 40 min. (Section S2, Table S2). This to obtain insight in the robustness of the proposed

280 method. The error on the repeatability of the retention times (n=3) was below 1% in all cases (and below

281 0.1% for 53% of the triplicate analyses) and hence in line with the expectations for HPLC.

282 Subsequently, the data was converted to RI. This such as to allow easier method transfer and instrument

283 independent model implementation. Although, this still imposes usage of the same stationary and

284 mobile phase and to some extent gradient slope, it does allow disconnection from the column

285 dimensions, flow rate, instrument and e.g., connection types used (Rigano et al., 2018). While the use

286 of linear RI is an established approach, strongly supporting the identification of unknowns in gas

287 chromatography, the field of HPLC has been mostly hindered by a lack of standardization on this issue.

288 The latter is partially driven by the aspect that the relationship between RI and the carbon number in

289 HPLC is quasilinear and not rectilinear as in GC (Rigano et al., 2018; Smith et al., 1987; Weitzel et al.,

290 2011). Due the more complex elution process in RPLC in which the compound hydrophobicity is the

291 main, but not the only, parameter controlling the elution, it is challenging, if not impossible, to identify

292 a homologues series of detectable solutes generally depicting a completely linear behaviour over the

293 entire elution range covered by the gradient. Problematic therein is that mere presence of a UV-

294 chromophore or API-MS compatible functional group in the calibration series affects linearity and  
295 hence limits the broadest possible implementation. Depending on the application in RPLC different  
296 types of calibration series have been proposed including alkan-2-ones, alkyl aryl ketones or 1-  
297 nitroalkenes (Baker, 1979; Baker and Ma, 1979; Bogusz and Aderjan, 1988; Bogusz and Wu, 1991;  
298 Smith, 1982). In this work the former ones are used (from 2-propanone to 2-dodecanone)(Baker and  
299 Ma, 1979). This because the alkyl aryl ketones comprise aromatic groups which are complicating the  
300 linearity between carbon number and retention. Also, the nitroalkenes are only incrementally useful  
301 for mapping the very polar solutes, a zone in which a hydrophobicity based predictive model is anyhow  
302 less performant (Baker and Ma, 1979; Bogusz and Aderjan, 1988; Smith, 1982). Because there has also  
303 been a lack of standardization in terms of the equation to be used to calculate the RI, the RI vs. carbon  
304 number plots were constructed for the alkan-2-ones ladder according to the various possible  
305 linearization methods (Figure S1). While none of the plots allows complete linearity it can be seen that  
306 over 90% of the plot excellent linearity is obtained and that only in the very low, below 2-butanone, or  
307 high retention regime, above 2-nonanone, a deviation is occurring. Considering that additionally  
308 linearity is a preferential but not an essential prerequisite for the use of RI, this data illustrates that use  
309 of RI in the proposed strategy and in RPLC is certainly a viable approach. Because several equations  
310 led to the same degree of linearity and/or the conventional gradient Kovats retention index Equation  
311 SE1 led to the highest correlation coefficient (0.97), to simplify the approach the latter was consequently  
312 used (Arigò et al., 2021).

### 313 **3.4 Selection of a model and descriptor types**

314 A QSRR method allows linking the molecular properties of an analyte to the chromatographic  
315 retention under given stationary and mobile phase conditions. Both linear models such as multiple linear  
316 regression (MLR) or Partial Least Squares regressions (PLS) or, nonlinear models, such as neural  
317 networks, have extensively been used for this purpose (Cirera-Domènech et al., 2013). ANN approach  
318 can be more flexible for modelling when using both linear and non-linear functions, but compared to  
319 MLR, the infrastructure is more complex (Ruggieri et al., 2005b). In the current work MLR modelling  
320 was selected as it allows obtaining robust, easy to reproduce via freely accessible software and therefore



321 more transferable, models. A retention relationship (a linear equation) is thereby constructed between  
322 a dependent variable (RI), and multiple independent variables, comprising a limited number of  
323 molecular descriptors. The identities and weight of the optimal descriptors are selected during the  
324 construction of the model. During model usage the actual value of each descriptor is then a priori  
325 calculated via software for each structural formula to allow subsequent retention time/index prediction  
326 by simple completion of the linear MLR equation. The contemporary availability of over 5000 chemo-  
327 informatics based molecular descriptors makes selection of the most suitable ones an increasingly  
328 challenging task, whereby models can easily lead to erroneous predictions when descriptor selection is  
329 suboptimal. Note that if too many of the available descriptors are used when creating a model, this does  
330 not lead to better and higher accuracy, but to overfitting, narrowing down the implementation range of  
331 the equation instead of making it generic (Sagandykova and Buszewski, 2021). A variety of 2-  
332 dimensional (2D), 3-dimensional (3D) molecular descriptors or other descriptors (such as scaffolds and  
333 fingerprint types) can today be directly obtained through online chemical databases. In order to allow  
334 selection from the broadest possible and most recent set of molecular descriptors available, in this work  
335 they were obtained through the AlvaDesc application. Therein 1879 descriptors were selected in the  
336 initial pool providing structural information such as molecular topology, flexibility, geometry.

### 337 **3.5 Optimized descriptors selection and model construction**

338 The MLR model construction and subsequent descriptor selection was performed through the  
339 VEGA ZZ software, which also allowed obtaining up-front model validation information. The initial  
340 screening of descriptors involved evaluating zero variance, which means removing any feature that has  
341 the same value for all the samples, as it does not add any information for the model. The second step  
342 involves conducting a single-variable regression analysis, which helps in identifying the features that  
343 are most relevant to the output variable, where poorly correlated ones were excluded ( $r^2 < 0.1$ ). 1800 of  
344 the 1879 descriptors were removed in this way as unable to contribute usefully to a combined MLR  
345 model. After conducting an evaluation of the variance inflation (VIF), it was determined that the  
346 remaining set contained collinear descriptors, leading to a reduction of the set to 37 relevant descriptors.  
347 The chemometrics used for feature selection in this study are commonly employed for high-dimensional

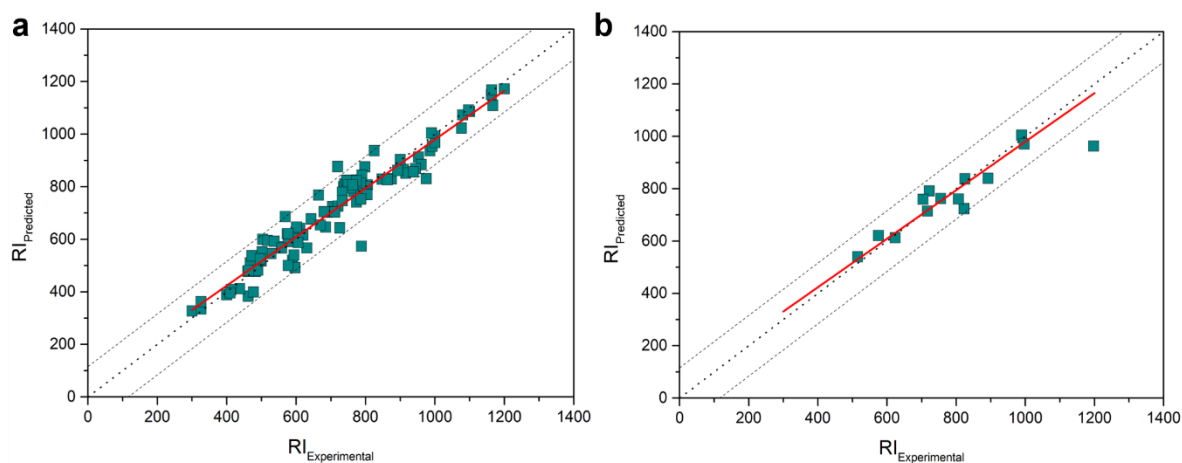
348 data to eliminate descriptors with no variation and identify strongly correlated descriptors, while more  
 349 advanced methods like principal component analysis, partial least squares, or random forest regression  
 350 may be needed to capture complex relationships and non-linear interactions between descriptors  
 351 (Danishuddin and Khan, 2016).

352 The most suitable MLR model was then obtained through the leave-one-out (LOO) optimization  
 353 algorithm, including calculation and ranking of the figures of merit of each possible equation. The most  
 354 excluded compound corresponded to a steroid testosterone undecanoate. The software itself allows  
 355 models with up to 8 regressors, and all were tested. Finally, the best-optimized model (n-1), depicting  
 356 a correlation  $r^2 = 0.93$ , was chosen comprising 7 variables, showing the lowest standard error of  
 357 prediction (SE=58). Another algorithm ( $r^2 = 0.90$ ) with 3 regressors was also observed and was suitable  
 358 for the same purposes of this work but with a slightly larger deviation (Equation SE2). Note that, using  
 359 high number of regressors can seemingly lead to enhanced models, but this could cause overfitting, and  
 360 hence lead to a less generically applicable model and errors. Furthermore, using a single global model  
 361 provides computational efficiency, simplified interpretation and implementation, versatility in handling  
 362 various analytes, and the ability to identify trends and patterns across multiple analytes, outweighing  
 363 the potential limitations of using local models and structurally similar training sets. In this way the  
 364 following Equation 1 was obtained allowing implementation for the predicting the RI values of all  
 365 possible hypothetically possible structural formulas for a given experimentally observed solute.

$$\begin{aligned}
 366 \quad RI_{predicted} = & 489.9565 + 358.6790 ALogPS_{logP} - 465.4977 ALogPS_{logS} - 249.3834 Psi_{i_A} + \\
 367 \quad & 465.8030 Chi_G + 304.7962 RBN + 150.6071 TDB06p + 144.8038 LOC \quad (1)
 \end{aligned}$$

368 The model comprises 7 descriptors from which 2 ALogPS (ALogPS\_logP and ALogPS\_logS) and  
 369 5 AlvaDesc (Psi\_i\_A, Chi\_G, RBN, TDB06p, and LOC). Unsurprisingly, a first descriptor selected  
 370 therein is *ALogPS\_logP*, representing the logarithm of the *n*-octanol/water partition coefficient. With a  
 371 correlation of  $r^2$  value of 0.78, in the single variable regression, it illustrates that indeed the hydrophobic  
 372 retention on a highly endcapped silica based C18 column is mostly, but not only, based on compound's  
 373 lipophilicity. Although, logD might be a more expected solution if other elements such as nitrogen were  
 374 also comprised, the full protonation of carboxylic groups under the used conditions ensures compound

375 neutrality and hence the same result as one would expect with logD, while allowing use of the simpler,  
376 and hence somewhat more robust logP calculations (Dong et al., 2009). *ALogPS\_logS*, another  
377 descriptor with high correlation value (0.63) represents aqueous solubility of a compound. As expected,  
378 more water soluble compounds proved less retained. Although, a collinearity with *ALogPS\_logP* could  
379 be reasonably expected, statistically this was not the case ( $VIF < 5$ ) (Sun, 2004). *Psi\_i\_A* (intrinsic state  
380 pseudoconnectivity index – type S average), a third descriptor of the model from a group of topological  
381 indices, with an  $r^2$  value of 0.62, was also withheld. These 2D descriptors (distance-, degree-, and  
382 spectrum-based), also known as connectivity indices, are based on the intrinsic and the  
383 electrotopological state values, which have shown beneficial correlations multiple times in literature  
384 when building QSAR, QSPR, or QSRR models (Chu et al., 2021; Ling et al., 2019). Furthermore, it  
385 was observed for *Chi\_G* (Randic-like index from geometrical matrix, a 3D matrix-based descriptor,  
386 with  $r^2=0.34$ ), that with increasing retention, the value drops. This descriptor could assist in  
387 distinguishing cyclic molecules (higher values) from more branched ones (lower values), as it contains  
388 the information of degree of branching as well as the molecular folding (Eichenlaub et al., 2022). The  
389 *RBN* (number of rotatable bonds) parameter, describes the number of any single bonds allowing the free  
390 rotation and is related to the size and flexibility of the molecule (Falcón-Cano et al., 2022). *TDB06p*  
391 (3D Topological distance based descriptors – lag 6 weighted by polarizability), a 3D autocorrelation  
392 type of descriptor,  $r^2=0.21$ , describing the shortest length distance between two atoms in a molecule  
393 with an emphasis to the polarizability of the molecule. Previous research showed that polarizability of  
394 a molecule can highly affect the elution order in RPLC (Andrade-Eiroa, 2011; Klein et al., 2004).  
395 Finally, the *LOC* (lopping centric index) descriptor belonging to the group of topological indices (with  
396 a correlation of 0.11) was the final descriptor selected in the model. Furthermore, it can represent the  
397 molecular branching degree, where the value increases with more branching graphs (Todeschini and  
398 Consonni, 2010; Yu, 2019).

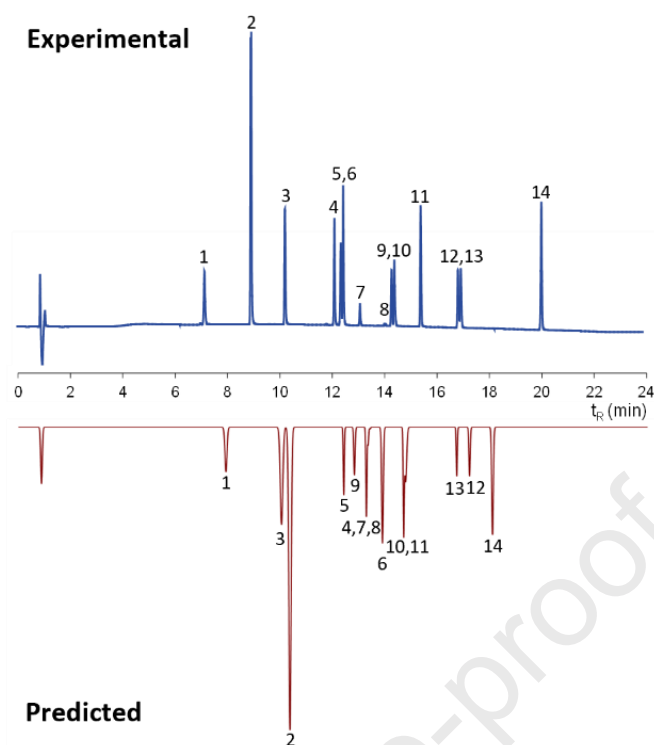


399

400 **Figure 3.** Linear fit displays RI predicted vs. RI experimental (a) for training set and (b) test set.

### 401 3.6 Model performance assessment with known environmentally relevant solutes

402 In Figure 3a the predicted RI as obtained via Equation 1 is represented versus the experimental RI  
 403 for all 101 compounds, delivering a plot depicting a correlation of  $r^2 = 0.93$ . Only 4% of data points did  
 404 not fit into  $\pm 2\sigma$ , and 74% fit  $\pm 1\sigma$ , where  $\sigma$  ( $SE=58$ ) is the standard deviation of the errors (Table S3).  
 405 In order to assess the predictive accuracy of the model with unrelated molecules from outside the  
 406 training set, it was subsequently tested with 14 compounds of environmental and pharmaceutical  
 407 relevance (Figure S3). An overlay of the thereby obtained predicted and experimental RI is shown in  
 408 Figure 3b, where obtained results fitted the 95% confidence margin, except one compound, 2,6-di-tert-  
 409 butyl-4-methyl phenol (BHT). The latter solute was, however, eluting after the latest eluting reference  
 410 compound from the ketone ladder (2-dodecanone), and is therefore too retained to fall into the  
 411 applicability range of the developed algorithm. The diverse test set were selected to span the molecular  
 412 space as represented in Figure 2. As can be seen in Figure 4 representing the experimental vs the  
 413 predicted retention (Table S8), 13 out of the 14 compounds meet the deviation margin, except for BHT  
 414 depicting a larger error due to above-mentioned reason. Although, for BHT, the real RI is impossible  
 415 to calculate, this was done by estimating the elution time of the next ketone elution in order. In general,  
 416 it can, thus be concluded that for solutes falling into the range for which the model was designed  
 417 (comprising only C, H, O,  $MW < 500$  and eluting between acetophenone and 2-dodecanone) that a  
 418 predictive deviation  $\pm 2\sigma$  or  $\pm 116$  RI is a realistic reliability threshold, which can be used in the structural  
 419 elucidation work (Section 3.7).



420

421 **Figure 4.** Overlay of the experimentally obtained retention of 14 solutes not used during the model  
 422 design with the predicted values. Peak identity: 1) phenol; 2) 2,7-dihydroxy naphthalene; 3) toluic acid;  
 423 4) propylparaben; 5) 1,3 butanediol diacrylate; 6) bisphenol A; 7) testosterone; 8) trans-2-hexenyl  
 424 acetate; 9) 3-tert-butyl-4-hydroxyanisole (BHA); 10) 4-ter-butyl benzoic acid; 11) diphenyl carbonate;  
 425 12) 4-hexylbenzoic acid; 13) butyl phenyl ether; 14) 2,6-di-tert-butyl-4-methyl phenol (BHT).

### 426 3.7 Implementation of the model to assist in de novo structural identification of unknown 427 solutes by RPLC-HRMS

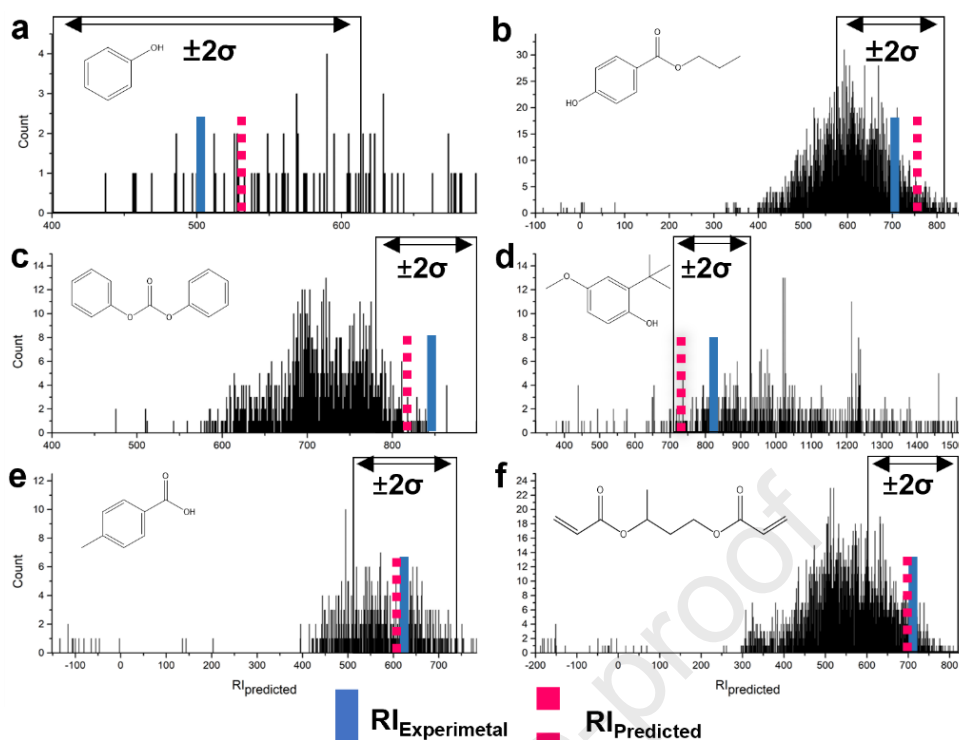
428 The actual goal of this work is to implement such models to support the structural elucidation  
 429 process of unknowns for which the elemental compositions and experimental retention times/indices  
 430 were obtained. The rationale is thereby that the developed model should be able to predict the retention  
 431 index of every hypothetical structural formula that can be drawn for a given elemental composition,  
 432 whereby the proposed structures eluting outside the  $\pm 2\sigma$  margin can be excluded upfront. The  
 433 challenges therein are the astronomical number of possible structures that can be drawn for a given  
 434 atomic composition and the current absence of embeddable algorithms allowing both generation of all  
 435 structures and incorporation in the proposed workflow. Another approach can be the use of the publicly  
 436 available libraries, which contain a number of possible known structures. While the former strategy is

437 ideally preferential, in order to demonstrate the current possibilities of the model, the proposed  
438 hypothetical structures were in this case obtained from the ChemSpider database (Pogliani, 2000).

439 This approach was tested with all 14 compounds used in section 3.6 and 6 out of 14 were presented  
440 in the text below: phenol, propylparaben, diphenyl carbonate, BHA, p-toluic acid and 1,3 butanediol  
441 diacrylate (for the remaining 8 solutes see Table S9). These were used as “unknowns”, for which  
442 predicted elemental compositions were obtained. Using ChemSpider as a database source, for the  
443 phenol case, the elemental composition ( $C_6H_6O$ ) led to 83 hypothetical structures. When plotting the  
444 corresponding RI for the obtained structures and definition of the  $\pm 116$  RI error margin zone above  
445 and below the experimental RI of the unknown (Figure 5a), it can be seen that only 17% of the proposed  
446 structures is eliminated. Specifically, the number of 83 possible structures thereby dropped to 69, one  
447 of which indeed corresponded to the predicted RI of phenol. The predicted RI (539) of the correct  
448 phenol structure thereby deviated 24 RI from the experimental value (515). While this illustrates that  
449 the proposed 1-D HPLC based predictive modelling method cannot on itself allow for sufficient attrition  
450 of all the incorrect structures, the proposed tool can be powerful in combination with the other available  
451 structural elucidation information. The structure of phenol can therefore, from the shortlisted of 69  
452 solutes, subsequently be obtained via e.g., mass (MS/MS) and UV spectrometric information, via  
453 comparison with standards, but also through chemical stability assessments (as most, if not all, of the  
454 non-aromatic hypothetical structures are highly reactive). The database delivered 3576 possible structural  
455 formulas for the elemental composition ( $C_{10}H_{12}O_3$ ) of propylparaben. It can be seen in Figure 5b that  
456 all structures deliver a RI  $<588$  and  $>820$ , after applying the model, elimination of the erroneous  
457 structures obtained was 42%. The left over indeed comprises the correct structure of propylparaben  
458 depicting a  $\Delta RI=55$  between the experimental (704) and predicted (759) RI value. In a fully analogous  
459 way, all RI for the possible structural formulas corresponding to  $C_{13}H_{10}O_3$  are represented in Figure 5c.  
460 Subsequent comparison with the experimental RI illustrates that the correct structure of diphenyl  
461 carbonate is included in a shortlist comprising only 136 of the 985 structures, corresponding to removal  
462 of 86% of the incorrect structures. Furthermore, Figure 5d shows another successful removal of 67%  
463 of impossible tentative structures for  $C_{11}H_{16}O_2$ , where 279 out of 849 remain for identification of BHA.

464 Somewhat less removal was obtained for p-toluic acid case,  $C_8H_8O_2$  (Figure 5e). Out of 582 possible  
465 structures generated, 28% can be eliminated. While the predictive accuracy for this solute is good  
466 ( $\Delta RI=12$ ) the large number of possible RI in the vicinity of the correct structures leaves the user with  
467 (too) many remaining possible solutions. Lastly, for the following elemental composition,  $C_{12}H_{18}O_4$ ,  
468 database comprised 2886 possible structural compositions. After applying a model, remaining 917 were  
469 left for further identification of 1,3 butanediol diacrylate allowing up to 68% of elimination (Figure 5f).

470 This limited number of examples illustrates the potential of the approach while proving the concept.  
471 A remaining hurdle with easy implementation of the ChromaRIM approach is the need to develop  
472 integrated software which can automatically generate all possible structures for a given atomic  
473 composition (or link to the public databases), calculate the corresponding descriptor values, generate  
474 the corresponding RI and eliminate all impossible (or at least improbable) ones in single automated  
475 procedure. While such integrated software is under development, the current work is mainly intending  
476 to introduce the principle, workflow, and an already applicable protocol to accept or exclude possible  
477 structures using ChromaRIM website (“Home page - ChromaRIM,” n.d.). It should be stressed that with  
478 the provided information the reader is already having all the required information to implement the tool  
479 for structural elucidation purposes. To assist this process, a user friendly standard operating procedure  
480 is therefore added with the supplementary information (section S5) to help the user in implementing the  
481 current model. Our website also contains an application allowing automated calculation of the RI based  
482 on the provided retention times, which will be further enhanced towards automated library search as  
483 this work is further progressing. Ideally in the future such an algorithm could be embedded in the LC-  
484 HRMS software for fully automated implementation.



485

486 **Figure 5.** Representation of the calculated RI for all obtained structures from ChemSpider for (a)  
 487 phenol, (b) propylparaben, (c) diphenyl carbonate, (d) 3-tert-butyl-4-hydroxyanisole (BHA), (e) p-  
 488 toluic acid, and (f) 1,3 butanediol diacrylate. The zone eliminated by a  $\pm 2\sigma$  or  $\pm 116$  RI deviation above  
 489 and below the experimental value of the elution time (converted to RI) is indicated together with the  
 490 experimental elution index and the predicted one for the correct structure.

#### 491 4. Conclusions

492 In this work a QSRR methodology is developed to assist in the structural elucidation of unknown  
 493 solutes composed of carbon, hydrogen, and oxygen with a molecular weight of up to a  $500 \text{ g mol}^{-1}$ . The  
 494 methodology was specifically developed to be instrument-independent and hence fully and easily  
 495 transferable and reproducible on any (U)HPLC-HRMS system. For this purpose, the predictive  
 496 algorithm was developed on a broadly used reversed phase column (Kinetex, core-shell C18) with  
 497 generic water/acetonitrile + 0.1% formic acid gradients covering the full range in elutropic strengths.  
 498 By data conversion to RI (with a ketone ladder) transferability is facilitated. An optimized multiple  
 499 linear regression-based model was developed based on the retention of 101 training solutes, whereby  
 500 an initial number of 1879 possible descriptors were screened. The latter were fine-tuned down to 7



501 remaining most influential descriptors in a linear equation allowing optimal prediction for all training  
502 solutes. This offers a model which can effectively be used for the prediction of the RI of unknowns  
503 within the predefined separation space. While, due to the sheer number of molecules in the latter is  
504 impossible to test the model with all solutes, the accuracy of the latter proved to allow correct RI  
505 prediction within a  $\pm 2\sigma$  range (mostly  $\pm 1\sigma$ ) for all test solutes not included in the training set and eluting  
506 within the ketone ladder. This suggest that broad implementation of the model is foreseeable. The  
507 applicability of the model is demonstrated through the correct elimination of large fractions of all  
508 possible structural formulas for a given elemental composition, effectively simulating the situation one  
509 would be confronted with when performing LC-HRMS. In all the six treated examples the model  
510 allowed correct elimination of a significant percentage of the incorrect structural formulas, whereby the  
511 RI of the correct structure was always within the remaining possible structures. The tool therefore  
512 appears applicable to support the identification of unknown C, H, O containing solutes  $< 500 \text{ g mol}^{-1}$ .

513

#### 514 **Author information**

##### 515 *Corresponding Author*

516 \* Frédéric Lynen

517 Tel: +32 (0) 9 264 9606; Fax: +32 (0) 9 264 4998.

518 E-mail: [frederic.lynen@ugent.be](mailto:frederic.lynen@ugent.be)

##### 519 *Author Contributions*

520 **Ardiana Kajtazi:** Conceptualization, Visualization, Methodology, Software, Investigation, Formal  
521 analysis, Writing - Original Draft; **Giacomo Russo:** Validation, Writing - Review & Editing; **Kristina**  
522 **Wicht:** Investigation; **Hamed Eghbali:** Supervision; **Frédéric Lynen:** Conceptualization,  
523 Visualization, Supervision, Writing - Review & Editing.

##### 524 **Acknowledgments**

525 We thank mag.ing.comp. Marin Kajtazi for assistance in developing the ChromaRIM software. This  
526 project has received funding from the European Union's EU Framework Programme for Research and

527 Innovation Horizon 2020 under Grant Agreement No 861369. (innoveox.eu). The FWO and the FNRS  
528 are acknowledged for funding part of this research through the Excellence of Science grant (30897864).

## 529 **References**

- 530 Aalizadeh, R., Alygizakis, N.A., Schymanski, E.L., Krauss, M., Schulze, T., Ibáñez, M., Mceachran,  
531 A.D., Chao, A., Williams, A.J., Gago-Ferrero, P., Covaci, A., Moschet, C., Young, T.M.,  
532 Hollender, J., Slobodnik, J., Thomaidis, N.S., 2021. Development and Application of Liquid  
533 Chromatographic Retention Time Indices in HRMS-Based Suspect and Nontarget Screening. *Cite*  
534 *This Anal. Chem* 93, 11601–11611. <https://doi.org/10.1021/acs.analchem.1c02348>
- 535 Aicheler, F., Li, J., Hoene, M., Lehmann, R., Xu, G., Kohlbacher, O., 2015. Retention Time Prediction  
536 Improves Identification in Nontargeted Lipidomics Approaches. *Anal. Chem.* 87, 7698–7704.  
537 <https://doi.org/10.1021/acs.analchem.5b01139>
- 538 Amos, R.I.J., Haddad, P.R., Szucs, R., Dolan, J.W., Pohl, C.A., 2018. Molecular modeling and  
539 prediction accuracy in Quantitative Structure-Retention Relationship calculations for  
540 chromatography. *TrAC - Trends Anal. Chem.* 105, 352–359.  
541 <https://doi.org/10.1016/j.trac.2018.05.019>
- 542 Andrade-Eiroa, A., 2011. Reverse-High Performance Liquid Chromatography Mechanism Explained  
543 by Polarization of Stationary Phase. *Chem* 1, 62–79. <https://doi.org/10.5618/chem.2011.v1.n1.8>
- 544 Arigò, A., Dugo, P., Rigano, F., Mondello, L., 2021. Linear retention index approach applied to liquid  
545 chromatography coupled to triple quadrupole mass spectrometry to determine oxygen heterocyclic  
546 compounds at trace level in finished cosmetics. *J. Chromatogr. A* 1649, 462183.  
547 <https://doi.org/10.1016/j.chroma.2021.462183>
- 548 Baker, J.K., 1979. Estimation of high pressure liquid chromatographic retention indices. *Anal. Chem.*  
549 51, 1693–1697. <https://doi.org/10.1021/ac50047a025>
- 550 Baker, J.K., Ma, C.Y., 1979. Retention index scale for liquid-liquid chromatography. *J. Chromatogr. A*  
551 169, 107–115. [https://doi.org/10.1016/0021-9673\(75\)85036-9](https://doi.org/10.1016/0021-9673(75)85036-9)
- 552 Bogusz, M., Aderjan, R., 1988. Improved standardization in reversed-phase high-performance liquid  
553 chromatography using 1-nitroalkanes as a retention index scale. *J. Chromatogr. A* 435, 43–53.

- 554 [https://doi.org/10.1016/S0021-9673\(01\)82161-0](https://doi.org/10.1016/S0021-9673(01)82161-0)
- 555 Bogusz, M., Wu, M., 1991. Standardized HPLC/DAD system, based on retention indices and spectral  
556 library, applicable for systematic toxicological screening. *J. Anal. Toxicol.* 15, 188–197.  
557 <https://doi.org/10.1093/jat/15.4.188>
- 558 Boiteau, R.M., Hoyt, D.W., Nicora, C.D., Kinmonth-Schultz, H.A., Ward, J.K., Bingol, K., 2018.  
559 Structure elucidation of unknown metabolites in metabolomics by combined NMR and MS/MS  
560 prediction. *Metabolites* 8. <https://doi.org/10.3390/metabo8010008>
- 561 Bouwmeester, R., Gabriels, R., Hulstaert, N., Martens, L., Degroeve, S., 2021. DeepLC can predict  
562 retention times for peptides that carry as-yet unseen modifications. *Nat. Methods* 2021 1811 18,  
563 1363–1369. <https://doi.org/10.1038/s41592-021-01301-5>
- 564 Chu, Y.M., Julietraja, K., Venugopal, P., Siddiqui, M.K., Prabhu, S., 2021. Degree- and irregularity-  
565 based molecular descriptors for benzenoid systems. *Eur. Phys. J. Plus* 2021 1361 136, 1–17.  
566 <https://doi.org/10.1140/EPJP/S13360-020-01033-Z>
- 567 Cirera-Domènech, E., Estrada-Tejedor, R., Broto-Puig, F., Teixidó, J., Gassiot-Matas, M., Comellas,  
568 L., Lliberia, J.L., Méndez, A., Paz-Estivill, S., Delgado-Ortiz, M.R., 2013. Quantitative structure–  
569 retention relationships applied to liquid chromatography gradient elution method for the  
570 determination of carbonyl-2,4-dinitrophenylhydrazone compounds. *J. Chromatogr. A* 1276, 65–  
571 77. <https://doi.org/10.1016/J.CHROMA.2012.12.027>
- 572 Codesido, S., Randazzo, G.M., Lehmann, F., González-Ruiz, V., García, A., Xenarios, I., Liechti, R.,  
573 Bridge, A., Boccard, J., Rudaz, S., 2019. DynaStI: A Dynamic Retention Time Database for  
574 Steroidomics. *Metab.* 2019, Vol. 9, Page 85 9, 85. <https://doi.org/10.3390/METABO9050085>
- 575 Cui, L., Lu, H., Lee, Y.H., 2018. Challenges and emergent solutions for LC-MS/MS based untargeted  
576 metabolomics in diseases. *Mass Spectrom. Rev.* 37, 772–792. <https://doi.org/10.1002/MAS.21562>
- 577 Danishuddin, Khan, A.U., 2016. Descriptors and their selection methods in QSAR analysis: paradigm  
578 for drug design. *Drug Discov. Today* 21, 1291–1302. <https://doi.org/10.1016/j.drudis.2016.06.013>
- 579 Datta, R., Das, D., Das, S., 2021. Efficient lipophilicity prediction of molecules employing deep-  
580 learning models. *Chemom. Intell. Lab. Syst.* 213, 104309.  
581 <https://doi.org/10.1016/j.chemolab.2021.104309>

- 582 De Vijlder, T., Valkenborg, D., Lemière, F., Romijn, E.P., Laukens, K., Cuyckens, F., 2018. A tutorial  
583 in small molecule identification via electrospray ionization-mass spectrometry: The practical art  
584 of structural elucidation. *Mass Spectrom. Rev.* 37, 607–629. <https://doi.org/10.1002/MAS.21551>
- 585 Domingo-Almenara, X., Guijas, C., Billings, E., Montenegro-Burke, J.R., Uritboonthai, W., Aisporna,  
586 A.E., Chen, E., Benton, H.P., Siuzdak, G., 2019. The METLIN small molecule dataset for machine  
587 learning-based retention time prediction. *Nat. Commun.* 2019 101 10, 1–9.  
588 <https://doi.org/10.1038/s41467-019-13680-7>
- 589 Dong, P.P., Ge, G.B., Zhang, Y.Y., Ai, C.Z., Li, G.H., Zhu, L.L., Luan, H.W., Liu, X.B., Yang, L.,  
590 2009. Quantitative structure-retention relationship studies for taxanes including epimers and  
591 isomeric metabolites in ultra fast liquid chromatography. *J. Chromatogr. A* 1216, 7055–7062.  
592 <https://doi.org/10.1016/J.CHROMA.2009.08.079>
- 593 Dorfer, V., Maltsev, S., Winkler, S., Mechtler, K., 2018. CharmeRT: Boosting Peptide Identifications  
594 by Chimeric Spectra Identification and Retention Time Prediction. *J. Proteome Res.* 17, 2581–  
595 2589. <https://doi.org/10.1021/acs.jproteome.7b00836>
- 596 Eichenlaub, J., Rakowska, P.W., Kloskowski, A., 2022. User-assisted methodology targeted for  
597 building structure interpretable QSPR models for boosting CO<sub>2</sub> capture with ionic liquids. *J. Mol.*  
598 *Liq.* 350, 118511. <https://doi.org/10.1016/J.MOLLIQ.2022.118511>
- 599 Eugster, P.J., Boccard, J., Debrus, B., Bréant, L., Wolfender, J.L., Martel, S., Carrupt, P.A., 2014.  
600 Retention time prediction for dereplication of natural products (C<sub>x</sub>H<sub>y</sub>O<sub>z</sub>) in LC-MS metabolite  
601 profiling. *Phytochemistry* 108, 196–207. <https://doi.org/10.1016/j.phytochem.2014.10.005>
- 602 Falcón-Cano, G., Molina, C., Cabrera-Pérez, M.Á., 2022. Reliable Prediction of Caco-2 Permeability  
603 by Supervised Recursive Machine Learning Approaches. *Pharm.* 2022, Vol. 14, Page 1998 14,  
604 1998. <https://doi.org/10.3390/PHARMACEUTICS14101998>
- 605 González-Ruiz, V., Olives, A.I., Martín, M.A., 2015. Core-shell particles lead the way to renewing  
606 high-performance liquid chromatography. *TrAC Trends Anal. Chem.* 64, 17–28.  
607 <https://doi.org/10.1016/J.TRAC.2014.08.008>
- 608 Gritti, F., 2023. Perspective on the Future Approaches to Predict Retention in Liquid Chromatography  
609 15, 39. <https://doi.org/10.1021/acs.analchem.0c05078>

- 610 Haddad, P.R., Taraji, M., Szücs, R., 2021a. Prediction of Analyte Retention Time in Liquid  
611 Chromatography. *Anal. Chem.* <https://doi.org/10.1021/acs.analchem.0c04190>
- 612 Haddad, P.R., Taraji, M., Szücs, R., 2021b. Prediction of Analyte Retention Time in Liquid  
613 Chromatography. *Anal. Chem.* 93, 228–256. <https://doi.org/10.1021/acs.analchem.0c04190>
- 614 Héberger, K., 2007. Quantitative structure–(chromatographic) retention relationships. *J. Chromatogr.*  
615 A 1158, 273–305. <https://doi.org/10.1016/j.chroma.2007.03.108>
- 616 Home page - ChromaRIM [WWW Document], n.d. URL <https://chromarim.ugent.be/> (accessed  
617 9.27.22).
- 618 Horai, H., Arita, M., Kanaya, S., Nihei, Y., Ikeda, T., Suwa, K., Ojima, Y., Tanaka, Kenichi, Tanaka,  
619 S., Aoshima, K., Oda, Y., Kakazu, Y., Kusano, M., Tohge, T., Matsuda, F., Sawada, Y., Hirai,  
620 M.Y., Nakanishi, H., Ikeda, K., Akimoto, N., Maoka, T., Takahashi, H., Ara, T., Sakurai, N.,  
621 Suzuki, H., Shibata, D., Neumann, S., Iida, T., Tanaka, Ken, Funatsu, K., Matsuura, F., Soga, T.,  
622 Taguchi, R., Saito, K., Nishioka, T., 2010. MassBank: a public repository for sharing mass spectral  
623 data for life sciences. *J. Mass Spectrom.* 45, 703–714. <https://doi.org/10.1002/JMS.1777>
- 624 Hutchins, P.D., Russell, J.D., Coon, J.J., 2018. LipiDex: An Integrated Software Package for High-  
625 Confidence Lipid Identification. *Cell Syst.* 6, 621–625.e5.  
626 <https://doi.org/10.1016/J.CELS.2018.03.011>
- 627 Kaliszan, R., 1993. Quantitative structure-retention relationships applied to reversed-phase high-  
628 performance liquid chromatography. *J. Chromatogr. A* 656, 417–435.  
629 [https://doi.org/10.1016/0021-9673\(93\)80812-M](https://doi.org/10.1016/0021-9673(93)80812-M)
- 630 Klein, C.T., Kaiser, D., Ecker, G., 2004. Topological Distance Based 3D Descriptors for Use in QSAR  
631 and Diversity Analysis. *J. Chem. Inf. Comput. Sci.* 44, 200–209.  
632 <https://doi.org/10.1021/CI0256236/ASSET/IMAGES/LARGE/CI0256236F00004.JPEG>
- 633 Köhler, H.-R., Gräff, T., Schweizer, M., Blumhardt, J., Burkhardt, J., Ehmann, L., Hebel, J., Heid, C.,  
634 Kundy, L., Kuttler, J., Malusova, M., Moroff, F.-M., Schlösinger, A.-F., Schulze-Berge, P.,  
635 Panagopoulou, E.I., Damalas, D.E., Thomaidis, N.S., Triebkorn, R., Maletzki, D., Kühnen, U.,  
636 von der Ohe, P.C., 2023. LogD-based modelling and  $\Delta\log D$  as a proxy for pH-dependent action  
637 of ionizable chemicals reveal the relevance of both neutral and ionic species for fish

- 638 embryotoxicity and possess great potential for practical application in the regulation of chemicals.  
639 Water Res. 235, 119864. <https://doi.org/10.1016/j.watres.2023.119864>
- 640 Kumari, S., Stevens, D., Kind, T., Denkert, C., Fiehn, O., 2011. Applying in-silico retention index and  
641 mass spectra matching for identification of unknown metabolites in accurate mass GC-TOF mass  
642 spectrometry. Anal. Chem. 83, 5895–5902. <https://doi.org/10.1021/ac2006137>
- 643 Ling, Y., Klemes, M.J., Steinschneider, S., Dichtel, W.R., Helbling, D.E., 2019. QSARs to predict  
644 adsorption affinity of organic micropollutants for activated carbon and B-cyclodextrin polymer  
645 adsorbents. Water Res. 154, 217–226. <https://doi.org/10.1016/J.WATRES.2019.02.012>
- 646 Liu, Y., Romijn, E.P., Verniest, G., Laukens, K., De Vijlder, T., 2019. Mass spectrometry-based  
647 structure elucidation of small molecule impurities and degradation products in pharmaceutical  
648 development. TrAC - Trends Anal. Chem. 121. <https://doi.org/10.1016/J.TRAC.2019.115686>
- 649 Ma, C., Ren, Y., Yang, J., Ren, Z., Yang, H., Liu, S., 2018. Improved Peptide Retention Time Prediction  
650 in Liquid Chromatography through Deep Learning. Anal. Chem. 90, 10881–10888.  
651 [https://doi.org/10.1021/ACS.ANALCHEM.8B02386/SUPPL\\_FILE/AC8B02386\\_SI\\_001.PDF](https://doi.org/10.1021/ACS.ANALCHEM.8B02386/SUPPL_FILE/AC8B02386_SI_001.PDF)
- 652 Majors, R., 2018. HPLC and UHPLC Columns: Then, Now, Next. LC-GC North Am. 36, 128–132.
- 653 Mauri, A., 2020. alvaDesc: A tool to calculate and analyze molecular descriptors and fingerprints.  
654 Methods Pharmacol. Toxicol. 801–820. [https://doi.org/10.1007/978-1-0716-0150-](https://doi.org/10.1007/978-1-0716-0150-1_32/FIGURES/3)  
655 [1\\_32/FIGURES/3](https://doi.org/10.1007/978-1-0716-0150-1_32/FIGURES/3)
- 656 Meshref, S., Li, Y., Feng, Y.L., 2020. Prediction of liquid chromatographic retention time using  
657 quantitative structure-retention relationships to assist non-targeted identification of unknown  
658 metabolites of phthalates in human urine with high-resolution mass spectrometry. J. Chromatogr.  
659 A 1634. <https://doi.org/10.1016/j.chroma.2020.461691>
- 660 Palmblad, M., RAMSTROM, M., BAILEY, C., MCCUTCHENMALONEY, S., BERGQUIST, J.,  
661 ZELLER, L., 2004. Protein identification by liquid chromatography–mass spectrometry using  
662 retention time prediction. J. Chromatogr. B 803, 131–135.  
663 <https://doi.org/10.1016/j.jchromb.2003.11.007>
- 664 Pedretti, A., Mazzolari, A., Gervasoni, S., Fumagalli, L., Vistoli, G., 2021. The VEGA suite of  
665 programs: An versatile platform for cheminformatics and drug design projects. Bioinformatics 37,

- 666 1174–1175. <https://doi.org/10.1093/bioinformatics/btaa774>
- 667 Pogliani, L., 2000. Modeling with molecular pseudoconnectivity descriptors. A useful extension of the  
668 intrinsic I-state concent. *J. Phys. Chem. A* 104, 9029–9045.  
669 <https://doi.org/10.1021/JP001191V/ASSET/IMAGES/MEDIUM/JP001191VU00015A.GIF>
- 670 Randazzo, G.M., Tonoli, D., Hambye, S., Guillarme, D., Jeanneret, F., Nurisso, A., Goracci, L.,  
671 Boccard, J., Rudaz, S., 2016a. Prediction of retention time in reversed-phase liquid  
672 chromatography as a tool for steroid identification. *Anal. Chim. Acta* 916, 8–16.  
673 <https://doi.org/10.1016/j.aca.2016.02.014>
- 674 Randazzo, G.M., Tonoli, D., Hambye, S., Guillarme, D., Jeanneret, F., Nurisso, A., Goracci, L.,  
675 Boccard, J., Rudaz, S., 2016b. Prediction of retention time in reversed-phase liquid  
676 chromatography as a tool for steroid identification. *Anal. Chim. Acta* 916, 8–16.  
677 <https://doi.org/10.1016/J.ACA.2016.02.014>
- 678 Rigano, F., Oteri, M., Russo, M., Dugo, P., Mondello, L., 2018. Proposal of a Linear Retention Index  
679 System for Improving Identification Reliability of Triacylglycerol Profiles in Lipid Samples by  
680 Liquid Chromatography Methods. *Anal. Chem.* 90, 3313–3320.  
681 <https://doi.org/10.1021/acs.analchem.7b04837>
- 682 Ruggieri, F., D'Archivio, A.A., Carlucci, G., Mazzeo, P., 2005a. Application of artificial neural  
683 networks for prediction of retention factors of triazine herbicides in reversed-phase liquid  
684 chromatography. *J. Chromatogr. A* 1076, 163–169. <https://doi.org/10.1016/j.chroma.2005.04.038>
- 685 Ruggieri, F., D'Archivio, A.A., Carlucci, G., Mazzeo, P., 2005b. Application of artificial neural  
686 networks for prediction of retention factors of triazine herbicides in reversed-phase liquid  
687 chromatography. *J. Chromatogr. A* 1076, 163–169.  
688 <https://doi.org/10.1016/J.CHROMA.2005.04.038>
- 689 Russo, G., Grumetto, L., Szucs, R., Barbato, F., Lynen, F., 2017. Determination of in Vitro and in Silico  
690 Indexes for the Modeling of Blood–Brain Barrier Partitioning of Drugs via Micellar and  
691 Immobilized Artificial Membrane Liquid Chromatography.  
692 <https://doi.org/10.1021/acs.jmedchem.6b01811>
- 693 Sagandykova, G., Buszewski, B., 2021. Perspectives and recent advances in quantitative structure-

- 694 retention relationships for high performance liquid chromatography. How far are we? *TrAC*  
695 *Trends Anal. Chem.* 141, 116294. <https://doi.org/10.1016/J.TRAC.2021.116294>
- 696 Smith, R.M., 1982. Alkylarylketones as a retention index scale in liquid chromatography. *J.*  
697 *Chromatogr. A* 236, 313–320. [https://doi.org/10.1016/S0021-9673\(00\)84880-3](https://doi.org/10.1016/S0021-9673(00)84880-3)
- 698 Smith, R.M., Murilla, G.A., Burr, C.M., 1987. Alkyl aryl ketones as a retention index scale with  
699 acetonitrile or tetrahydrofuran containing eluents in reversed-phase high-performance liquid  
700 chromatography. *J. Chromatogr. A* 388, 37–49. [https://doi.org/10.1016/S0021-9673\(01\)94464-4](https://doi.org/10.1016/S0021-9673(01)94464-4)
- 701 Sun, H., 2004. A Universal Molecular Descriptor System for Prediction of LogP, LogS, LogBB, and  
702 Absorption. <https://doi.org/10.1021/ci030304f>
- 703 Szucs, R., Brown, R., Brunelli, C., Heaton, J.C., Hradski, J., 2021. Structure Driven Prediction of  
704 Chromatographic Retention Times: Applications to Pharmaceutical Analysis. *Int. J. Mol. Sci.* 22,  
705 3848. <https://doi.org/10.3390/ijms22083848>
- 706 Tanaka, N., Mccalley, D. V., 2015. Core–Shell, Ultrasmall Particles, Monoliths, and Other Support  
707 Materials in High-Performance Liquid Chromatography.  
708 <https://doi.org/10.1021/acs.analchem.5b04093>
- 709 Tetko, I. V., Gasteiger, J., Todeschini, R., Mauri, A., Livingstone, D., Ertl, P., Palyulin, V.A.,  
710 Radchenko, E. V., Zefirov, N.S., Makarenko, A.S., Tanchuk, V.Y., Prokopenko, V. V., 2005.  
711 Virtual computational chemistry laboratory--design and description. *J. Comput. Aided. Mol. Des.*  
712 19, 453–463. <https://doi.org/10.1007/S10822-005-8694-Y>
- 713 Tiwary, S., Levy, R., Gutenbrunner, P., Salinas Soto, F., Palaniappan, K.K., Deming, L., Berndl, M.,  
714 Brant, A., Cimermanic, P., Cox, J., 2019. High-quality MS/MS spectrum prediction for data-  
715 dependent and data-independent acquisition data analysis. *Nat. Methods* 2019 166 16, 519–525.  
716 <https://doi.org/10.1038/s41592-019-0427-6>
- 717 Todeschini, R., Consonni, V., 2010. Molecular Descriptors for Chemoinformatics, Molecular  
718 Descriptors for Chemoinformatics. <https://doi.org/10.1002/9783527628766>
- 719 Virtual Computational Chemistry Laboratory [WWW Document], n.d. URL <http://www.vcclab.org/>  
720 (accessed 9.27.22).
- 721 Weitzel, K., Chemie, F., Rev, M.S., Introduction, I., Reference, C., 2011. Bond-Dissociation Energies



- 722 of Cations — Pushing the. WHO Libr. Cat. Data 221–235. <https://doi.org/10.1002/mas>
- 723 Wen, Y., Amos, R.I.J., Talebi, M., Szucs, R., Dolan, J.W., Pohl, C.A., Haddad, P.R., 2019. Retention  
724 prediction using quantitative structure-retention relationships combined with the hydrophobic  
725 subtraction model in reversed-phase liquid chromatography. *Electrophoresis* 40, 2415–2419.  
726 <https://doi.org/10.1002/elps.201900022>
- 727 Wen, Y., Amos, R.I.J., Talebi, M., Szucs, R., Dolan, J.W., Pohl, C.A., Haddad, P.R., 2018a. Retention  
728 Index Prediction Using Quantitative Structure-Retention Relationships for Improving Structure  
729 Identification in Nontargeted Metabolomics. *Anal. Chem.* 90, 9434–9440.  
730 <https://doi.org/10.1021/acs.analchem.8b02084>
- 731 Wen, Y., Talebi, M., Amos, R.I.J., Szucs, R., Dolan, J.W., Pohl, C.A., Haddad, P.R., 2018b. Retention  
732 prediction in reversed phase high performance liquid chromatography using quantitative structure-  
733 retention relationships applied to the Hydrophobic Subtraction Model. *J. Chromatogr. A* 1541, 1–  
734 11. <https://doi.org/10.1016/j.chroma.2018.01.053>
- 735 Witting, M., Böcker, S., 2020. Current status of retention time prediction in metabolite identification.  
736 *J. Sep. Sci.* 43, 1746–1754. <https://doi.org/10.1002/jssc.202000060>
- 737 Xu, Z., Chughtai, H., Tian, L., Liu, L., Roy, J.F., Bayen, S., 2023. Development of quantitative  
738 structure-retention relationship models to improve the identification of leachables in food  
739 packaging using non-targeted analysis. *Talanta* 253. <https://doi.org/10.1016/j.talanta.2022.123861>
- 740 Yang, Q., Ji, H., Lu, H., Zhang, Z., 2021. Prediction of Liquid Chromatographic Retention Time with  
741 Graph Neural Networks to Assist in Small Molecule Identification. *Anal. Chem.*  
742 <https://doi.org/10.1021/acs.analchem.0c04071>
- 743 Yu, X., 2019. Prediction of Depuration Rate Constants for Polychlorinated Biphenyl Congeners. *ACS*  
744 *Omega* 4, 15615–15620.  
745 [https://doi.org/10.1021/ACSOMEGA.9B02072/ASSET/IMAGES/MEDIUM/AO9B02072\\_M01](https://doi.org/10.1021/ACSOMEGA.9B02072/ASSET/IMAGES/MEDIUM/AO9B02072_M01)  
746 0.GIF
- 747 Zheng, S.J., Liu, S.J., Zhu, Q.F., Guo, N., Wang, Y.L., Yuan, B.F., Feng, Y.Q., 2018. Establishment of  
748 Liquid Chromatography Retention Index Based on Chemical Labeling for Metabolomic Analysis.  
749 *Anal. Chem.* 90, 8412–8420. <https://doi.org/10.1021/acs.analchem.8b00901>

**Highlights**

- Chromatographic Retention Index Model (ChromaRIM) in RPLC-HRMS
- Structural elucidation of small environmental solutes assisted by developed model
- Supporting unknown identification of  $C_xH_yO_z$  molecules < 500 Da
- The model implementation was demonstrated with 6 relevant compounds
- Elimination of a significant % of the incorrect structural formulas was achieved

Journal Pre-proof

**Declaration of interests**

The authors declare that they have no known competing financial interests or personal relationships that could have appeared to influence the work reported in this paper.

The authors declare the following financial interests/personal relationships which may be considered as potential competing interests:

Journal Pre-proof